One-Neutron Removal Measurement Reveals ^{24}O as a New Doubly Magic Nucleus

R. Kanungo,[1,*] C. Nociforo,[2] A. Prochazka,[2,3] T. Aumann,[2] D. Boutin,[3] D. Cortina-Gil,[4] B. Davids,[5] M. Diakaki,[6]
F. Farinon,[2,3] H. Geissel,[2] R. Gernhäuser,[7] J. Gerl,[2] R. Janik,[8] B. Jonson,[9] B. Kindler,[2] R. Knöbel,[2,3] R. Krücken,[7]
M. Lantz,[9] H. Lenske,[3] Y. Litvinov,[2] B. Lommel,[2] K. Mahata,[2] P. Maierbeck,[7] A. Musumarra,[10,11] T. Nilsson,[9] T. Otsuka,[12]
C. Perro,[1] C. Scheidenberger,[2] B. Sitar,[8] P. Strmen,[8] B. Sun,[2] I. Szarka,[8] I. Tanihata,[13] Y. Utsuno,[14]
H. Weick,[2] and M. Winkler[2]

[1]*Astronomy and Physics Department, Saint Mary's University, Halifax, NS B3H 3C3, Canada*
[2]*GSI Helmholtzzentrum für Schwerionenforschung, D-64291 Darmstadt, Germany*
[3]*Justus-Liebig University, 35392 Giessen, Germany*
[4]*Universidad de Santiago de Compostela, E-15706 Santiago de Compostella, Spain*
[5]*TRIUMF, Vancouver, British Columbia V6T 2A3, Canada*
[6]*National Technical University, Athens, Greece*
[7]*Physik Department E12, Technische Universität München, D-85748 Garching, Germany*
[8]*Faculty of Mathematics and Physics, Comenius University, 84215 Bratislava, Slovakia*
[9]*Chalmers University of Technology, Göteborg, SE 412-916, Sweden*
[10]*Universita' di Catania, 95153 Catania, Italy*
[11]*INFN-Laboratori Nazionali del Sud, 95123 Catania, Italy*
[12]*Center for Nuclear Study, University of Tokyo, Wako Shi, Saitama 351-0198, Japan*
[13]*RCNP, Osaka University, Mihogaoka, Ibaraki, Osaka 567 0047, Japan*
[14]*Japan Atomic Energy Agency, Tokai, Ibaraki 319-1195, Japan*
(Received 8 November 2008; published 13 April 2009)

The first measurement of the momentum distribution for one-neutron removal from ^{24}O at $920A$ MeV performed at GSI, Darmstadt is reported. The observed distribution has a width (FWHM) of 99 ± 4 MeV/c in the projectile rest frame and a one-neutron removal cross section of 63 ± 7 mb. The results are well explained with a nearly pure $2s_{1/2}$ neutron spectroscopic factor of 1.74 ± 0.19 within the eikonal model. This large s-wave probability shows a spherical shell closure thereby confirming earlier suggestions that ^{24}O is a new doubly magic nucleus.

Nuclei far from stability have presented a more general view of nuclear structure that is inaccessible with stable nuclei. One of the major changes to our conventional concept is the modification of nuclear shell structure. Mass measurements and Coulomb excitation measurements of neutron-rich Na and Mg isotopes suggested the breakdown of the traditional magic number $N = 20$ [1–3]. This raised questions on whether nuclear shell structure completely dissolves at the limits of stability. However, a new shell closure at $N = 16$ was pointed out through the systematical trends of one-neutron separation energies [4]. Further systematics of beta decay Q values, neutron and proton separation energies [5] suggested that ^{24}O could be a new doubly magic nucleus with both $N = 16$ and $Z = 8$ showing features of magic numbers in this region. These observations provided empirical signatures for the $N = 16$ magic number. To establish ^{24}O as a doubly closed shell nucleus, spectroscopic information is required to determine the spherical nature of the shell closure. The first experiment in this direction establishing this fact is reported here.

The $N = 16$ shell gap has been suggested to arise [6] due to an upward shift of the $d_{3/2}$ orbital as an effect of the $(\sigma \cdot \sigma)(\tau \cdot \tau)$ interaction [7]. In-beam gamma spectros-copy suggested that the excited states for ^{23,24}O are un-bound [8]. The unbound $(3/2^{+})$ excited state for ^{23}O [9] was found to be 4 MeV above the ground state while a $(5/2^{+})$ excited state has been observed at 2.8(1) MeV excitation energy [10]. The ground state of ^{23}O has been suggested to have a spin of $1/2^{+}$ from momentum distri-bution and Coulomb dissociation studies [11–13]. The two-neutron removal momentum distribution measure-ment suggested that in ^{23}O two-neutrons maybe occupying the $2s_{1/2}$ orbital [14]. Recently, the size of the $N = 16$ shell gap in ^{25}O was determined to be 4.86(13) MeV from the observed resonance for this unbound nucleus using invari-ant mass spectroscopy [15].

The drip line for the oxygen isotopes is reached at the $N = 16$ isotope ^{24}O, while the conventionally expected doubly closed shell nucleus ^{28}O [16] as well as ^{26}O [17,18] have been found to be unbound. Evidence for a shell closure at $N = 16$ therefore would suggest that ^{24}O is a new doubly closed shell nucleus. The confirmation of a spherical shell closure can be found from the neutron occupancies in ^{24}O; however, the available spectroscopic information is very limited.

In this Letter we report on the first measurement to obtain the occupation number of the orbitals in ^{24}O. The

momentum distribution from one-neutron removal is highly sensitive to the single-particle orbital(s) occupied by the valence neutrons. Our results show that the valence neutrons in ^{24}O dominantly reside in the $2s_{1/2}$ orbital. This observation proves a spherical shell closure in ^{24}O.

The experiment was performed at the fragment separator FRS [19] at GSI, Germany. The ^{24}O secondary beam was produced via projectile fragmentation of a ^{48}Ca beam at $1A$ GeV interacting with a 6.347 g/cm^2 thick Be target placed at the entrance of the FRS. The nuclei produced were then separated and identified event by event using the first half of the FRS, with the magnetic rigidity ($B\rho$), energy loss (ΔE) and time-of-flight (TOF) information.

Figure 1 shows a schematic view of the experimental setup at the FRS. The first three focal planes ($F1$-$F3$) of the FRS are dispersive and the fourth ($F4$) is achromatic. A 4.05 g/cm^2 thick carbon reaction target was placed at $F2$. Three plastic scintillators of 3, 3.5, and 5 mm thicknesses were located at the $F1$, $F2$, and $F4$ foci, respectively. The time of flight before the reaction target was measured using two plastic scintillator detectors placed at $F1$ and $F2$.

The charge (Z) of incident nuclei in front of the reaction target was measured using a multisampling ionization chamber [20]. The chamber has eight anodes from which the signals were read out independently and could be summed and averaged in the offline analysis. The 1 standard deviation resolution ($\Delta E/E$) achieved with the summed signal for oxygen ions was 3.3%.

The incident nuclei were tracked using two time projection chambers (TPCs) [21]. The position resolutions were $\sigma_x \sim 130$ μm and $\sigma_y \sim 65$ μm. The tracking allowed the determination of the position of the beam on the reaction target. The rate of ^{24}O nuclei impinging on the reaction target was around 3 pps.

Behind the reaction target the outgoing fragments were tracked using two TPC detectors placed just downstream of the reaction target. The ^{23}O fragments were then trans-ported to the final achromatic focus $F4$ using the second half of the fragment separator as a high resolution spectrometer. At $F4$ the fragments were identified using the same experimental method of $B\rho$-ΔE-TOF. The TOF was measured with the plastic scintillators at $F2$ and $F4$. Two multisampling ionization chambers were placed at $F4$ to identify the charge of the fragments through energy loss. The fragment position at the focus was determined by tracking the particles through two TPC detectors located at $F4$. The image position of the target in the horizontal (x) direction at $F4$ was determined from the correlation of position and angle of the fragment at $F4$.

The FRS was operated in a dispersion matched (achromatic) mode where the momentum broadening of the incident beam (^{24}O) at the production target is not contributing to the final image size at $F4$. In this mode the dispersion of the first half of the FRS is matched by its second half (i.e., from $F2$ to $F4$). This results in an achromatic focus at $F4$. Therefore, the additional momentum broadening caused by the reaction in the secondary target at $F2$, is measured in the position distribution at $F4$ without the influence of the momentum spread at the entrance of the FRS.

The energy loss in and the shape of the reaction target at $F2$ leads to some deviation from this ideal achromatic image conditions as observed through a correlation of the x position at the reaction target at $F2$ and the position at $F4$ focus. The position at $F2$ is mainly determined by the momentum distribution of the incident beam. This correlation could then be corrected to improve the achromatic condition by making the position at $F4$ independent of that at $F2$.

The momentum distribution due to the one-neutron removal reaction in the laboratory was obtained from the measured position distribution at the $F4$ focus (x_4) corrected to restore the achromatic condition and applying the dispersion relation (D_{24}) of the second half of the FRS
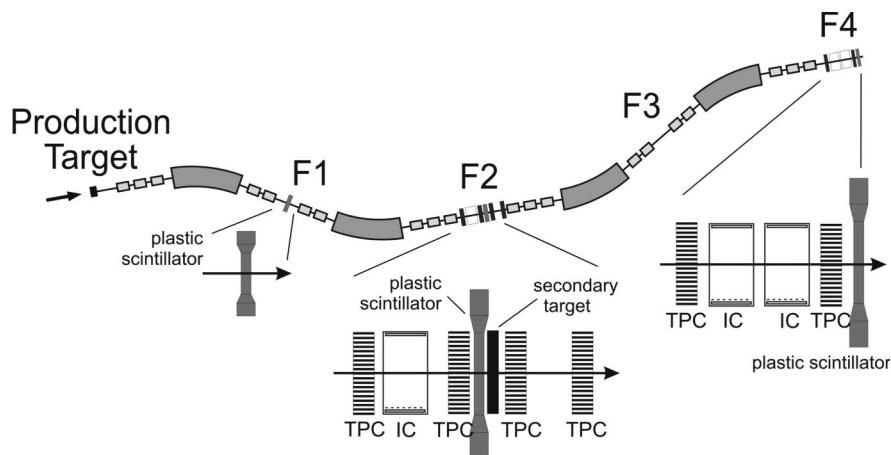

FIG. 1. Schematic setup of the experiment on precise momentum measurements of ^{23}O fragments after neutron removal in a secondary target placed at the central focal plane of the FRS, GSI.

through the relation

$$P_f^{\text{lab}} = \left(1 + \frac{x_4}{D_{24}}\right) z_f B\rho, \qquad (1)$$

where z_f is the atomic number of the fragment and $B\rho$ is the magnetic rigidity of the central rays with which the FRS is operated. To obtain the longitudinal momentum distribution in the projectile rest frame we have to perform the Lorentz transformation given by the relation

$$P_\| = \gamma_b(P_f^{\text{lab}} - \beta_b E_f^{\text{lab}}). \qquad (2)$$

For this purpose, one needs to know the velocity of the beam (β_b) at the point of interaction. This was found at the midtarget location using the time of flight before the target from $F1$ to $F2$ which was calibrated using a primary beam of ^{48}Ca with known energies.

The resolution for the momentum distribution was measured by transporting the unreacted ^{24}O beam to $F4$ after penetration through the reaction target. The momentum resolution is shown by the open circles in Fig. 2. Its width (FWHM) was found to be 33 MeV/c when fitted with a Gaussian distribution. The momentum distribution for one-neutron removal ^{24}O → ^{23}O is shown by the filled circles in Fig. 2. This distribution when fitted with a Gaussian function has a width of 99 ± 4 MeV/c (FWHM). The momentum resolution is shown normalized to the peak of the ^{24}O → ^{23}O momentum distribution to allow for a comparison of the widths.

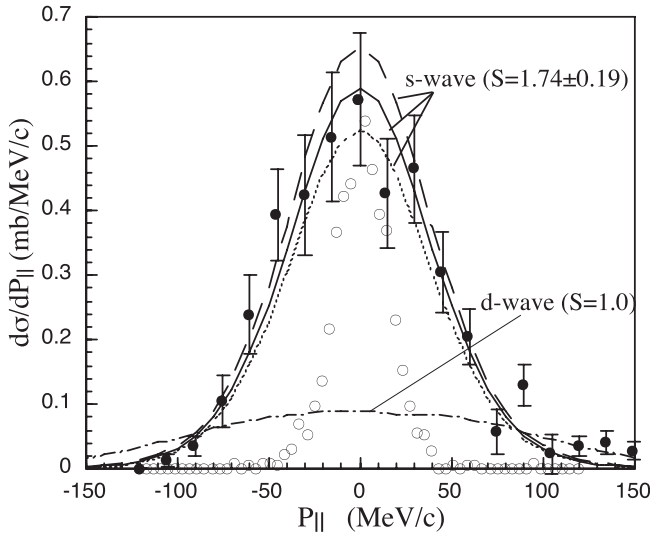The background originating from the residual matter (detectors in air) at the central focal plane was separately

FIG. 2. The longitudinal momentum distribution data for ^{24}O → ^{23}O (filled circles) and the momentum resolution (open circles). The dash-dotted line shows the calculated distribution for neutron knocked out from $1d_{5/2}$ orbital. The solid, dashed, and dotted lines show calculated distributions for neutrons removed from $2s_{1/2}$ orbital with $S = 1.74$, 1.93, 1.55, respectively.

measured without the breakup target inserted. To subtract the background, the number of ^{23}O fragments detected without the secondary target were normalized by the ratio of the incident beam (^{24}O) counts measured with and without target. The filled circles in Fig. 2 show the background subtracted data. The measured one-neutron removal cross section is 63 ± 7 mb. Effects of optical transmission losses as well as those due to reactions in the material have been taken into account. The error bars include statistical errors as well as systematic errors from the target thickness measured to be 1.2%, and from transmission simulations estimated to 10%.

To extract the information on the spectroscopic factor(s) of the valence neutron in ^{24}O, we compare the measured momentum distribution both in shape and magnitude with eikonal model predictions. This model is based on a core + n description of ^{24}O. In this description we consider the configuration ^{23}O$_{gs}(1/2^+)$ + n in the $2s_{1/2}$ orbital as well as ^{23}O$_{gs}(5/2^+)$ + n in the $1d_{5/2}$ orbital.

The curves in Fig. 2 show the results of eikonal model calculations, folded with the experimental resolution, within the few-body Glauber theory [22] based on the above mentioned core+neutron model of ^{24}O. The neutron wave functions for the $2s_{1/2}$ and $1d_{5/2}$ orbitals were obtained by solving the Schrödinger equation with a Woods-Saxon potential. The depth of the potential was adjusted to reproduce the one-neutron separation energy of ^{24}O. The one-neutron separation energy (S_n) of ^{24}O is 3.61 ± 0.27 MeV [23]. The ^{23}O core density is of harmonic oscillator form that reproduces the measured interaction cross section of ^{23}O.

The calculation for the configuration with ^{23}O$_{gs}$ + $n(1d_{5/2})$ is shown as the dash-dotted line (Fig. 2). This is seen to be clearly much wider than the observed distribution. The calculated distribution for the configuration with ^{23}O$_{gs}$ + $n(2s_{1/2})$ (solid line) well reproduces the observed distribution. The spectroscopic factor (S) for the neutrons in the $2s_{1/2}$ orbital is therefore obtained from a best fit normalization of the ^{23}O$_{gs}$ + $n(2s_{1/2})$ momentum distribution to the data through chi-square minimization yielding $S = 1.74 ± 0.19$. The error bar represents 1 standard deviation error from the chi-square minimum. In Fig. 2 the solid line shows the best fit to the data, while the dashed line and the dotted line are the 1 standard deviation upper and lower error bands of the spectroscopic factor, respectively. The calculated single-particle cross section, i.e., with $S = 1$, for one-neutron removal from the $2s_{1/2}$ orbital is 34 mb which is multiplied by $S = 1.74 ± 0.19$ while comparing to the measured value.

The large spectroscopic factor observed for the $2s_{1/2}$ orbital implies that the single-particle strength of the valence neutron is strongly concentrated in the $2s_{1/2}$ state. Therefore there must be a large gap between the $2s_{1/2}$ and the $1d_{3/2}$ orbitals, as otherwise the strength in the $2s_{1/2}$ state would be reduced by the possibility of other single-

TABLE I. Spectroscopic factors for $^{24}O \rightarrow {}^{23}O$ and energies of levels in ^{23}O using the SDPF-M and USDB interactions compared to that obtained from this experiment.

Spin	SDPF-M Energy (MeV)	SDPF-M C^2S	USDB Energy (MeV)	USDB C^2S	Exp S
$1/2^+$	0.0	1.769	0.0	1.810	1.74(19)
$5/2^+$	2.586	5.593	2.593	5.665	

particle components in the ground state. This is consistent with the shell gap at $N = 16$. The strong s-wave probability shows for the first time the shell closure to be a spherical one, thereby establishing that ^{24}O is a new doubly closed shell nucleus.

We performed shell-model calculations for comparison with the spectroscopic factors obtained in the present experiment. The results are summarized in Table I. The theoretical spectroscopic factor is denoted by C^2S. In an extreme single-particle model $C^2S(2s_{1/2})$ should be 2 and $C^2S(1d_{5/2})$ should be 6. In this work we adopt the SDPF-M interaction [6,24], which is defined for the full sd shell and $1f_{7/2} + 2p_{3/2}$ orbits and gives an excellent description of the disappearance of the $N = 20$ magic number around ^{32}Mg. Since for oxygen isotopes the dimensions of the shell-model Hamiltonian are small enough to carry out exact diagonalization, eigenstates are calculated using the shell-model code OXBASH [25] without truncating the model space. For comparison spectroscopic factors calculated using the USDB [26] sd-shell interaction are presented as well.

The one-neutron separation energy for ^{23}O predicted by the SDPF-M interaction is 2.597 MeV while that using the USDB interaction is 2.581 MeV. Experimentally, ^{23}O is bound by 2.74(13) MeV. The energy of the $5/2^+$ state in ^{23}O is predicted to be slightly bound using the SDPF-M interaction, being only 11 keV below the neutron threshold, but it is unbound by 12 keV with the USDB interaction. Experimentally the possible location of the $5/2^+$ state is reported to be 45 keV above the neutron threshold [10]. According to the predicted large spectroscopic factor for the $5/2^+$ state (Table I) the d-wave component can be expected to be visible in this experiment if the state was bound. The data, however, do not show any significant d-wave component thereby suggesting the unbound nature of the $5/2^+$ state.

The good agreement between the predicted spectroscopic factor using the SDPF-M interaction and the present experiment is supportive of the description including the pf model space. Even though the pf shell comes down close to the $d_{3/2}$ orbit, the $N = 16$ shell closure is still stiff. Within the experimental errors, the predictions from USDB interaction are consistent as well.

In summary, we report here the first investigation of the valence neutron spectroscopic factor in ^{24}O through the one-neutron removal reaction measured at $920A$ MeV. The measured momentum distribution has a Gaussian width of 99 ± 4 MeV/c (FWHM). A comparison with eikonal model calculations shows that the distribution is predominantly described by neutrons in the $2s_{1/2}$ orbital with a spectroscopic factor of 1.74 ± 0.19. This value is in good agreement with SDPF-M as well as USDB shell model calculations and establishes the spherical shell closure at $N = 16$ in ^{24}O making it a new doubly magic nucleus.

*ritu@triumf.ca
[1] C. Thibault *et al.*, Phys. Rev. C **12**, 644 (1975).
[2] T. Motobayashi *et al.*, Phys. Lett. B **346**, 9 (1995).
[3] B. V. Pritychenko *et al.*, Phys. Lett. B **461**, 322 (1999).
[4] A. Ozawa *et al.*, Phys. Rev. Lett. **84**, 5493 (2000).
[5] R. Kanungo *et al.*, Phys. Lett. B **528**, 58 (2002).
[6] Y. Utsuno *et al.*, Phys. Rev. C, **60**, 054315 (1999).
[7] T. Otsuka *et al.*, Phys. Rev. Lett. **87**, 082502 (2001).
[8] M. Stanoiu *et al.*, Phys. Rev. C **69**, 034312 (2004).
[9] Z. Elekes *et al.*, Phys. Rev. Lett. **98**, 102502 (2007).
[10] A. Schiller *et al.*, Phys. Rev. Lett. **99**, 112501 (2007).
[11] D. Cortina-Gil *et al.*, Phys. Rev. Lett. **93**, 062501 (2004).
[12] E. Sauvan *et al.*, Phys. Rev. C **69**, 044603 (2004).
[13] C. Nociforo *et al.*, Phys. Lett. B **605**, 79 (2005).
[14] R. Kanungo *et al.*, Phys. Rev. Lett. **88**, 142502 (2002).
[15] C. R. Hoffman *et al.*, Phys. Rev. Lett. **100**, 152502 (2008).
[16] H. Sakurai *et al.*, Phys. Lett. B **448**, 180 (1999).
[17] D. Guillemaud-Mueller *et al.*, Phys. Rev. C **41**, 937 (1990).
[18] A. Schiller *et al.*, Phys. Rev. C **72**, 037601 (2005).
[19] H. Geissel *et al.*, Nucl. Instrum. Methods Phys. Res., Sect. B **70** 286 (1992).
[20] A. Stolz *et al.*, Phys. Rev. C **65**, 064603 (2002).
[21] V. Hlinka *et al.*, Nucl. Instrum. Methods Phys. Res., Sect. A **419**, 503 (1998).
[22] Y. Ogawa *et al.*, Nucl. Phys. A **571**, 784 (1994).
[23] G. Audi *et al.*, Nucl. Phys. A **729**, 337 (2003).
[24] Y. Utsuno *et al.*, Phys. Rev. C **70**, 044307 (2004).
[25] B. A. Brown, A. Etchegoyen, and W. D. M. Rae, MSU-NSCL Report No. 524, 1986.
[26] B. A. Brown and W. A. Richter, Phys. Rev. C **74**, 034315 (2006).